

Basic Study

Association of colorectal cancer with pathogenic *Escherichia coli*: Focus on mechanisms using optical imaging

Julie Veziant, Johan Gagnière, Elodie Jouberton, Virginie Bonnin, Pierre Sauvanet, Denis Pezet, Nicolas Barnich, Elisabeth Miot-Noirault, Mathilde Bonnet

Julie Veziant, Johan Gagnière, Virginie Bonnin, Pierre Sauvanet, Denis Pezet, Nicolas Barnich, Mathilde Bonnet, UMR1071 Inserm/Université d'Auvergne and INRA USC2018, Clermont Université, 63000 Clermont-Ferrand, France

Julie Veziant, Johan Gagnière, Pierre Sauvanet, Denis Pezet, Service de Chirurgie Digestive, Centre Hospitalier Universitaire, 63000 Clermont Ferrand, France

Elodie Jouberton, Elisabeth Miot-Noirault, UMR990 Inserm/Université d'Auvergne, Clermont Université, 63000 Clermont-Ferrand, France

Elodie Jouberton, Service de Médecine Nucléaire, Centre Jean Perrin, 63000 Clermont Ferrand, France

Author contributions: Veziant J, Gagnière J, Bonnet M conceived and designed the study, analyzed data and drafted the manuscript; Veziant J, Jouberton E, Bonnin V, Bonnet M performed experiments and analyses; Miot-Noirault E contributed to imaging platform management; Sauvanet P performed histological techniques; Gagnière J, Pezet D, Barnich N, Miot-Noirault E and Bonnet M contributed to critical comments and revised the manuscript; all authors read, contributed to, and approved the final manuscript.

Supported by Veziant J was supported by «année-recherche» grants from the Ministère de la Santé and the Faculté de Médecine de Clermont-Ferrand; Gagnière J was supported by a “Nuovo Soldati Foundation for Cancer Research” grant.

Institutional review board statement: Not concerned.

Institutional animal care and use committee statement: The studies were performed in accordance with the French Regional Ethical Animal Use Committee (No. CEEA-02).

Conflict-of-interest statement: No.

Data sharing statement: Not concerned.

Open-Access: This article is an open-access article which was selected by an in-house editor and fully peer-reviewed by external

reviewers. It is distributed in accordance with the Creative Commons Attribution Non Commercial (CC BY-NC 4.0) license, which permits others to distribute, remix, adapt, build upon this work non-commercially, and license their derivative works on different terms, provided the original work is properly cited and the use is non-commercial. See: <http://creativecommons.org/licenses/by-nc/4.0/>

Correspondence to: Dr. Mathilde Bonnet, PhD, UMR1071 Inserm/Université d'Auvergne and INRA USC2018, Clermont Université, 28 Place Henri Dunant, 63000 Clermont-Ferrand, France. mathilde.bonnet@udamail.fr
Telephone: +33-4-73178381
Fax: +33-4-73178381

Received: June 24, 2015

Peer-review started: June 28, 2015

First decision: October 8, 2015

Revised: February 29, 2016

Accepted: March 24, 2016

Article in press: March 25, 2016

Published online: June 10, 2016

Abstract

AIM: To investigate the molecular or cellular mechanisms related to the infection of epithelial colonic mucosa by *pkcs*-positive *Escherichia coli* (*E. coli*) using optical imaging.

METHODS: We choose to evaluate the tumor metabolic activity using a fluorodeoxyglucose analogue as 2-deoxyglucosone fluorescent probes and to correlate it with tumoral volume (mm³). Inflammation measuring myeloperoxidase (MPO) activity and reactive oxygen species production was monitored by a bioluminescent (BLI) inflammation probe and related to histological examination and MPO levels by enzyme-linked immunosorbent assay (ELISA) on tumor specimens. The detection and quantitation of these two signals were

validated on a xenograft model of human colon adenocarcinoma epithelial cells (HCT116) in nude mice infected with a *pks*-positive *E. coli*. The inflammatory BLI signal was validated intra-digestively in the colitis-CEABAC10 DSS models, which mimicked Crohn's disease.

RESULTS: Using a 2-deoxyglucosone fluorescent probe, we observed a high and specific HCT116 tumor uptake in correlation with tumoral volume ($P = 0.0036$). Using the inflammation probe targeting MPO, we detected a rapid systemic elimination and a significant increase of the BLI signal in the *pks*-positive *E. coli*-infected HCT116 xenograft group ($P < 0.005$). ELISA confirmed that MPO levels were significantly higher (1556 ± 313.6 vs 234.6 ± 121.6 ng/mL $P = 0.001$) in xenografts infected with the pathogenic *E. coli* strain. Moreover, histological examination of tumor samples confirmed massive infiltration of *pks*-positive *E. coli*-infected HCT116 tumors by inflammatory cells compared to the uninfected group. These data showed that infection with the pathogenic *E. coli* strain enhanced inflammation and ROS production in tumors before tumor growth. Moreover, we demonstrated that the intra-digestive monitoring of inflammation is feasible in a reference colitis murine model (CEABAC10/DSS).

CONCLUSION: Using BLI and fluorescence optical imaging, we provided tools to better understand host-pathogen interactions at the early stage of disease, such as inflammatory bowel disease and colorectal cancer.

Key words: Colorectal carcinoma; *Escherichia coli*; Colibactin; Myeloperoxidase; *In vivo* optical imaging

© **The Author(s) 2016.** Published by Baishideng Publishing Group Inc. All rights reserved.

Core tip: Approximately 15% of cancers are related to infectious agents. Colorectal cancer (CRC) is thus a complex association of non-neoplastic and tumoral cells and a large amount of microorganisms. Recent studies reported that *pks*-positive *Escherichia coli* (*E. coli*) strains are more frequently detected in CRC, suggesting their possible role in tumor development. Optical imaging has emerged as a powerful tool in translational cancer research, providing new possibilities for the spatiotemporal monitoring of carcinogenesis in mouse models. It may be particularly helpful in better understanding the *in vivo* host-pathogen-interactions in tumor development. This is the first study to use optical imaging to explore CRC carcinogenesis and associated pathogenic *E. coli*.

Veizant J, Gagnière J, Jouberton E, Bonnin V, Sauvanet P, Pezet D, Barnich N, Miot-Noirault E, Bonnet M. Association of colorectal cancer with pathogenic *Escherichia coli*: Focus on mechanisms using optical imaging. *World J Clin Oncol* 2016; 7(3): 293-301 Available from: URL: <http://www.wjgnet.com/2218-4333/full/v7/i3/293.htm> DOI: <http://dx.doi.org/10.5306/wjco.v7.i3.293>

INTRODUCTION

Colorectal cancer (CRC) is the third most frequently diagnosed cancer worldwide^[1]. Despite recent advances in therapeutic care, CRC remains the second cause of cancer-related death after lung neoplasia and is responsible for over 600000 deaths annually^[1,2]. It is a multifactorial disease, strongly associated with genetic and environmental factors that favor tumor development^[3]. Approximately 15% of cancers can be related to infectious agents^[4,5], such as *Helicobacter pylori* (*H. pylori*) and gastric cancer^[6]. Colorectal cancer thus involves a complex association of non-neoplastic and tumoral cells and a large amount of microorganisms. Gut microbiota, a bacterial community of over 100 trillion microbial cells, plays a major role in colorectal carcinogenesis. Indeed, high bacterial density in the colon (10^{12} commensal bacteria/g of intestinal contents) compared to the small intestine (10^2 commensal bacteria/g of intestinal contents) is correlated with a higher risk of cancer development^[7]. Gut microbiota dysbiosis has recently been linked to CRC^[8-13], and several bacteria are involved in colorectal carcinogenesis, such as *Streptococcus bovis*^[14,15], *Enterococcus* spp.^[16], *H. pylori*^[17-19], *Bacteroides fragilis*^[20,21], *Clostridium septicum*^[22], *Fusobacterium* spp.^[23,24] and *Escherichia coli* (*E. coli*)^[25,26].

E. coli is a commensal bacteria of the human gut microbiota that plays a major role in maintaining intestinal homeostasis^[27]. Some strains became pathogenic, carrying virulence factors and producing toxins, such as cyclomodulins. These toxins can affect differentiation, apoptosis, and cell proliferation by interfering with the eukaryotic cell cycle and/or inducing DNA damage. Particularly, one of these toxins, the colibactin, is encoded by the *pks* genomic island and can lead to the creation of double-strand DNA breaks and thus induce the chromosomal instability involved in CRC^[28,29]. Recent studies reported that *pks*-positive *E. coli* is more frequently detected in CRC patients, suggesting a possible role in tumor development^[30-32]. Various independent studies showed that *pks*-positive-*E. coli* exhibit procarcinogenic properties in murine models, such as the multiple intestinal neoplasia (Min) mice model^[33], azoxymethane (AOM)-treated *IL10*^{-/-} mice^[34] and AOM/DSS models^[26]. Thereby, some pathogenic *E. coli* strains involved in colon carcinogenesis are now emerging. Nevertheless, mechanisms of action remain to be clarified, particularly in *in vivo* models.

The aim of the present study was to investigate *in vivo* the molecular or cellular mechanisms related to the infection of epithelial mucosa by *pks*-positive *E. coli* using 2D optical imaging. Indeed, optical imaging is emerging as a new powerful sensitive technology for the non-invasive spatiotemporal visualization of carcinogenesis in mice models, and it may help to better understand the host-pathogen interactions in colorectal tumor development^[35-37]. Because chronic inflammation and reactive oxygen species (ROS) production are

key factors in bacteria and CRC interactions, we chose to evaluate *pks*-positive *E. coli* infection on these mechanisms using commercial, available and validated probes^[31,38-40]. Indeed, inflammation could play a key role in the development of dysbiosis related to CRC^[40]. *E. coli* is also the most characterized bacteria associated with inflammatory bowel disease, which is a known risk factor for CRC^[41,42]. Moreover, Raisch *et al.*^[38] demonstrated that *E. coli* in colon cancer induces a significant increase in COX-2 expression in macrophages, the predominant type of immune cell that infiltrates tumors. Moreover, macrophages and other immune cells infiltrate the tumors, release myeloperoxidase (MPO), and produce ROS by several chemical reactions. Arthur *et al.*^[31,39] investigated *in vivo* the complex interplay between inflammation, bacteria and carcinogenesis and suggested that chronic inflammation is essential for tumor development by maintaining the expression of *pks* island genes. ROS production has also been reported in many suspected mechanisms related to CRC development. Neutrophils and macrophages, which are present in inflamed tissues such as colon tumors, are major providers of ROS. Maddocks *et al.*^[40,43] described a possible interaction between *E. coli* and the DNA repair system with elevated ROS levels. Because ROS oxidizes the luminescent probe and thus produces proportional light that is detectable *in vivo* with an optical imager^[44,45], we choose to monitor the inflammatory pathway and ROS production using on a bioluminescent (BLI) approach. The monitoring of inflammation was first performed and validated on a colitis murine model (CEABAC10/DSS mice). Then, by this approach, we showed, on a xenograft murine model, that *pks*-positive-*E. coli* significantly induces oxidative stress and inflammation before stimulating HCT116-tumor growth. While monitoring longitudinal inflammation, we choose to assess tumor growth by determining tumor metabolic activity with a fluorescent tool based on the fluorodeoxyglucose analogue 2-deoxyglucosone.

MATERIALS AND METHODS

Animal models

Studies were performed in accordance with the French Regional Ethical Animal Use Committee (No. CEEA-02). All mouse models were housed in specific pathogen-free conditions (22 ± 2 °C, 50% humidity, 12 h light/12 h dark) in the animal care facility of the Université d'Auvergne, Clermont-Ferrand, France.

HCT116 xenograft models

The HCT116 colorectal cancer cells were maintained as monolayers in culture flasks using culture medium consisting of McCoy's 5a Medium (Modified) supplemented with 10% FCS (Biowest, Nuaille, France), 2 mmol/L glutamine and 1% antibiotics. All the cells were grown at 37 °C in a humidified incubator

containing 5% CO₂.

Xenografts of human CRC were induced in male nude mice (Swiss nu/nu), weighting 26-33 g at the time of injection (7 wk old, Charles Rivers). We excluded female nude mice in order to avoid a possible hormonal influence. A total of 10 male nude mice were divided into two groups: Non-infected control xenograft (*n* = 5) and *pks*-positive *E. coli*-infected xenograft (*n* = 5). According to the infected xenograft, HCT116 cells were mixed with *pks*-positive *E. coli* as previously described by Cougnoux *et al.*^[34]. Beforehand, bacteria were grown at 37 °C in Luria-Bertani medium. *Pks*-positive *E. coli* is an ampicillin- and kanamycin-resistant *E. coli* strain named 11G5, isolated from a patient presenting with colon cancer and previously presented by Bonnet *et al.*^[33]. We used human colon adenocarcinoma epithelial cells (HCT116) to establish the xenograft models.

Then, animals anesthetized by isoflurane inhalation were inoculated with 2 × 10⁶ HCT116 cells embedded in growth factor-reduced Matrigel (Becton Dickinson) by dorsal subcutaneous injection at day 0 of the experiment.

Tumor size was assessed two times per week and tumor volume was obtained according to the following formula: (width² × length)/2 = *V* (mm³). The longest diameter (*L*) and maximum diameter (*W*) perpendicular to the direction of the longest diameter were determined using a caliper. Mice were sacrificed at 35 d post-injection, and the xenograft was collected from all animals and subjected to histologic examination and enzyme-linked immunosorbent assay (ELISA).

Colitis-CEABAC10 DSS models

Six CEABAC10 transgenic mice in an *in vivo* model mimicking colitis and Crohn's disease^[46] were used to monitor intra-digestive inflammation. They were divided into two groups. Mice from the same generation were used for experimentation. One group (*n* = 3) received one cycle of dextran sodium sulfate (DSS) in drinking water for 6 d at 1% (DSS-treated mice group) as described previously in Denizot *et al.*^[46]. The other group received only drinking water (*n* = 3; DSS-).

Optical imaging

For both BLI and fluorescence imaging acquisition, all animals were imaged using a dedicated high-sensitivity peltier-cooled (-90 °C) backlit charge-coupled device camera (IVIS Spectrum®, Perkin Elmer, United States). All acquisitions were performed under the same exposure conditions according to fluorescence or BLI imaging, with acquisition settings (binning and duration) set up depending upon the signal at the time of acquisition.

Prior to imaging, animals were anesthetized with 2%-3% isoflurane in an induction chamber; then, 2% isoflurane in air/O₂ was continuously delivered *via* a nose cone system in the dark box of the imaging system (delivered gas to up to 5 mice). To limit auto-

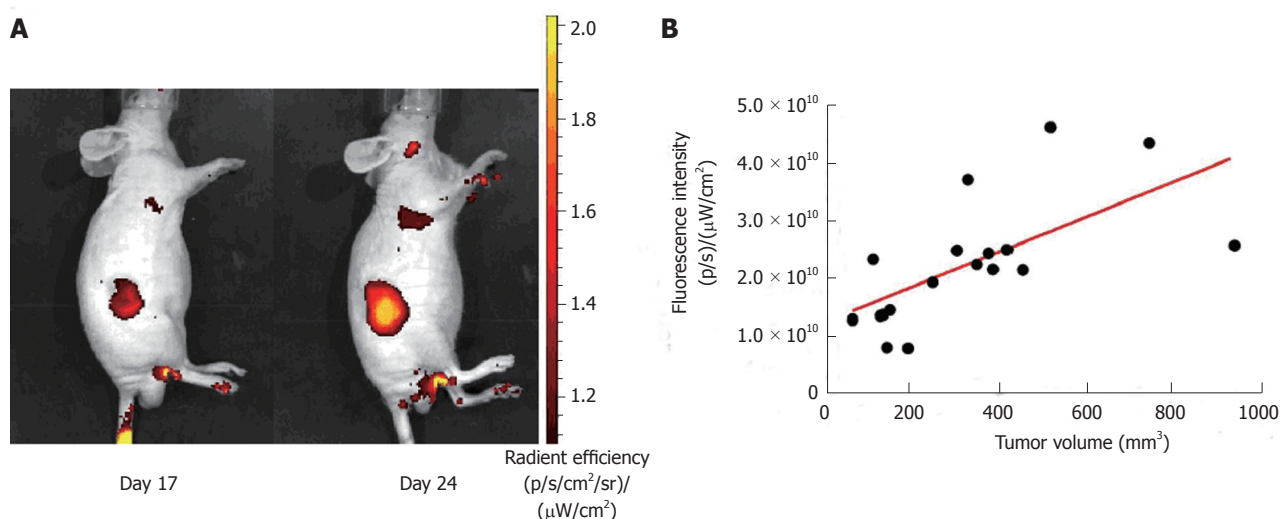


Figure 1 Correlation of tumor volume (HCT116 cells xenograft) and 2-DG-750 fluorescence signal uptake. A: Representative animal images showing the increase in fluorescence signal intensity with tumor development (day 17 and day 24 post-xenograft); B: Correlation between tumor development determined using a caliper and increase in fluorescence signal intensity (Pearson's correlation factor $r = 0.4197$; $P = 0.0036$).

fluorescence related to melanin, mice were shaved before all imaging procedures (except nude mice, which are hairless).

We used the XénoLight Rediject 2-DG-750 fluorescent probe or the XénoLight Rediject Inflammation chemiluminescent probe (Perkin Elmer, United States) to monitor metabolic activity or inflammation (MPO and ROS detection), respectively.

To monitor inflammation in HCT116-grafted nude mice at 20 d and 34 d post-xenograft, we administered by intraperitoneal (i.p.) injection of 150 μL of the XenoLight Rediject Inflammation probe per mouse. Mice were then imaged 10 min post-injection (exposure time of 5 min). In the colitis CEABAC10 model, imaging was performed 6 d after the DSS cycle. To monitor inflammation at depth and limit the decrease of the BLI signal intensity in this model, we administered by an intravenous (i.v.) injection of 150 μL/mouse. With i.v. injection, the best time to image the animal was immediately post-injection (exposure time of 5 min).

For tumor metabolic activity, we administered by an intravenous injection of 100 μL/mouse and imaged them 3 h after 2-DG-750 probe injection using one filter set (excitation: 745 nm, emission: 820 nm) and a high-throughput epi-illumination acquisition mode. All nude mice were imaged individually at 17 d and 24 d post-xenograft.

Quantitative analysis of imaging was performed using Living Image® Software (Caliper Life Science, United States) with the region of interest delineated manually over organs exhibiting probe accumulation. Every image series had the same scales, set manually, to facilitate the visual comparison of signal intensity at each time point. For the BLI signal, photon flux was expressed as the average radiance in p/s/cm²/sr. Fluorescence emission was also normalized to photons per second per centimeter squared per steradian (p/s/cm²/sr).

Histological analysis

After mouse sacrifice, tumor pieces were fixed in formol solution. Paraffin-embedded sections were cut into 5-μm slices, and tissue sections were prepared for hematoxylin-eosin-safran staining and routine pathological analysis with focus on the mitotic index, infiltrating cells and tumor necrosis. Sample preparations and observations were made in the Centre Imagerie Cellulaire Santé platform (Clermont-Ferrand).

MPO activity determination

After mouse sacrifice, tumor pieces were frozen in liquid nitrogen and stored at -80 °C until used. We performed an enzyme-linked immunosorbent assay to determine the levels of MPO (ng/mL) in all the tumors according to the manufacturer's instructions (R and D systems). Data were standardized on whole protein extracts stained with Coomassie blue.

Statistical analysis

Graph Pad Prism 5 STATA (StataCorp) was used for all statistical analysis. Unpaired Student's *t* test was used for the comparisons of the 2 groups. We determined the Pearson's correlation coefficient *r* to assess the degree of correlation. We considered *P* values of < 0.05 to be statistically significant.

RESULTS

Metabolic activity of the CRC xenograft model

In HCT116-grafted nude models, we confirmed a rapid systemic elimination of the 2-deoxyglucosone fluorescent probe with a very weak whole body uptake 180 min after probe-injection (Figure 1A). Moreover, a high and specific HCT116 tumor uptake was evidenced for each tumor 17 and 34 d post-graft. We demonstrated an increase of signal intensity over time, reflecting tumor growth. The tumor uptake of the

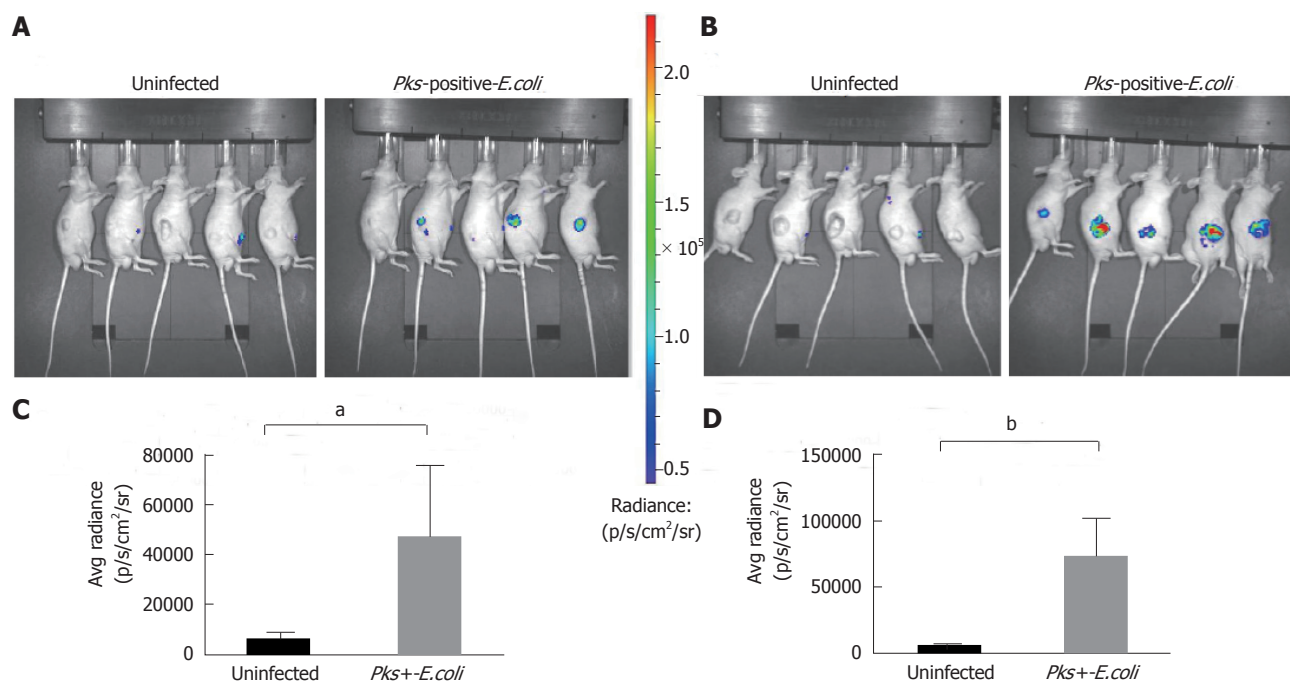


Figure 2 Significant increase of inflammation in HCT116 tumors infected with *Escherichia coli* strains measured by optical imaging using the inflammation probe. *In vivo* BLI imaging was performed at day 20 (A) and day 34 (B) post-HCT116 xenograft in nude mice ($n = 5$ animals with uninfected xenograft; $n = 5$ animals in *pks*-positive *E. coli*-infected xenograft). BLI images comparing uninfected to *pks*-positive *E. coli*-infected xenografts are shown on day 20 (A) and day 34 (B) post-xenograft. Intensity of emission is represented as the pseudocolor image. A sharp increase in the BLI signal was seen in the *pks*-positive *E. coli*-infected xenograft group at each time point. The BLI signal detected 10 min after i.p. probe injection was quantified from the ROI drawn manually. Photon flux was expressed as the average radiance in p/s/cm²/sr. Graphs reveal a statistically significant increase in the BLI signal in the *pks*-positive *E. coli*-infected tumors: day 20, ^a $P = 0.0132$ (C) and day 34, ^b $P = 0.0006$ (D). BLI: Bioluminescent; *E. coli*: *Escherichia coli*; i.p.: Intraperitoneal.

2-deoxyglucosone fluorescent signal was significantly ($P = 0.0036$) correlated with tumor volume, as determined using a caliper (Figure 1B). The *in vivo* monitoring of HCT116 tumor growth by the 2-deoxyglucosone fluorescent probe was efficient. No difference in tumor uptake was observed between uninfected and *pks*-positive *E. coli*-infected HCT116 cells (data not shown), as previously described with caliper determination by Cougnoux *et al.*^[34] at 34 d post-xenograft.

We tested 2-deoxyglucosone fluorescent imaging on Colitis-CEABAC10 DSS models. We did not observe any fluorescent signal *in vivo* in mice, reflecting that the targeting probe is specific for tumor cells (data not shown).

***Pks*-positive *E. coli* *in vivo* induces inflammation in the CRC xenograft model**

Using the inflammation probe, all nude mice were imaged 20 and 34 d post-xenograft. We detected a rapid systemic elimination in all mice and a strong BLI signal in HCT116 tumors in the infected group 10 min after probe injection (Figure 2A and B). Figure 2A and B clearly show that the intensity of the BLI signal (average radiance in p/s/cm²) was stronger in xenografts infected with the pathogenic *pks*-positive *E. coli* strain compared to uninfected ones at each time point investigated (20 and 34 d post-xenograft). Quantitation confirmed a significant increase of the BLI signal in the infected tumors 20 d ($P = 0.0132$, Figure 2C) and 34 d ($P =$

0.0006, Figure 2D) after the xenograft.

Monitoring intra-digestive BLI signals in Colitis-CEABAC10 DSS models

Then, we analyzed the monitoring of intra-digestive BLI signals using the inflammation probe in the CEABAC10 colitis mouse model. We induced intra-digestive inflammation using DSS in the first group, while control mice received only drinking water. To visualize BLI imaging in deep tissues *in vivo* in mice, the probe was injected intravenously. DSS group imaging showed a high BLI signal in DSS animals, reflecting severe intra-digestive inflammation (DSS+) relative to the untreated group (DSS-) (Figure 3). We demonstrated that monitoring intradigestive inflammation with the BLI signal is feasible and consistent.

Histological characterization

The histologic analysis of tumor samples indicated and confirmed that tumor cells in *pks*-positive *E. coli*-infected xenografts were surrounded by a remarkable infiltration of activated phagocytes (Figure 4C and D) compared to the uninfected group (Figure 4A and B). In addition, tumor necrosis was observed, especially in the *pks*-positive *E. coli*-infected group (Figure 4C). Moreover, HCT116 are characterized by megalocytosis and the progressive enlargement of the cell body and nucleus in *pks*-positive *E. coli*-infected xenografts. Histological examination confirmed the data from BLI

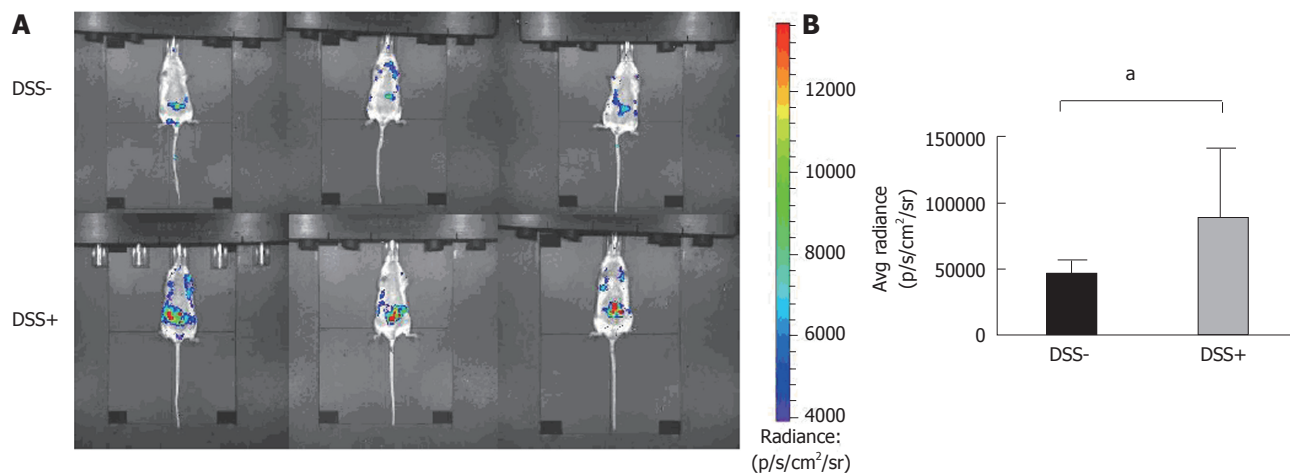


Figure 3 Monitoring of intra-digestive bioluminescent signals using the inflammation probe in the CEABAC10 mouse model. One mouse group was treated with 1% dextran sodium sulfate (DSS-treated mice group) in drinking water for 6 d ($n = 3$), while the other group received only drinking water ($n = 3$; DSS-). Mice were subjected to one cycle of DSS and then imaging with the inflammation probe before sacrifice. Mice were intravenously injected with the inflammation probe, and the BLI signal was detected immediately after injection. DSS-treated mouse group acquisition (A) showed severe intra-digestive inflammation was correlated with a significant increase in the BLI signal on graphs (B) compared to the DSS group ($^*P = 0.03$). BLI: Bioluminescent; DSS: Dextran sodium sulfate.

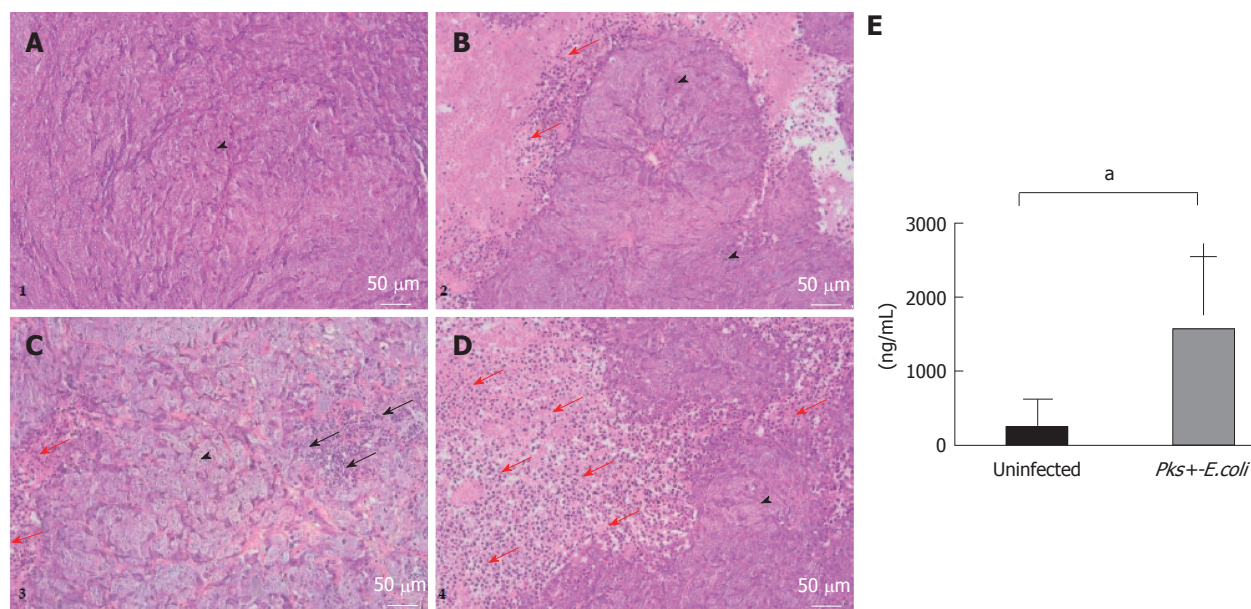


Figure 4 Histological and molecular analyses of HCT116 tumor samples. A-D: Histological examination of representative HCT116 tumor samples. Xenografts were harvested, paraffin embedded and processed for hematoxylin/eosin/safran. A and B are representative histological examinations from the uninfected xenograft group. C and D are representative histological examinations from the *pks*-positive-*E. coli* infected xenograft group. We noted that HCT116 tumor cells (arrowheads) infected with pathogenic *E. coli* strains are characterized by megalocytosis and progressive enlargement of the cell body and nucleus. Tumor cells in the *pks*-positive *E. coli*-infected xenograft group were surrounded by a remarkable infiltration of inflammatory cells (red arrow) compared to the uninfected xenograft group. Tumor necrosis was observed, especially in the infected xenograft group (black arrow). (Scale bars: $50 \mu\text{m} \times 20$); E: MPO levels by enzyme-linked immunosorbent assay (ELISA) on HCT116 tumor specimens. An ELISA test was performed on tumor specimens after mouse sacrifice (day 34 post-xenograft). MPO standardized levels were significantly higher (1556 ± 313.6 vs 234.6 ± 121.6 , $^*P = 0.001$) in xenografts infected with pathogenic *pks*-positive *E. coli* strains. *E. coli*: *Escherichia coli*; MPO: Myeloperoxidase.

imaging (inflammation probe).

MPO levels by ELISA

To confirm the quantitation of inflammation imaging, we assessed MPO activity on HCT116-xenograft-tumor specimens by performing an ELISA. MPO levels (ng/mL) were significantly higher (1556 ± 313.6 vs 234 ± 121.6 , $P = 0.001$) in xenografts infected with the *pks*-positive *E. coli* strain. These results showed

that the pathogenic *E. coli* strain enhanced MPO release compared to uninfected xenografts and confirmed the data from BLI imaging.

DISCUSSION

Optical imaging appears to be a powerful, highly sensitive tool in translational cancer research, providing new possibilities for *in vivo* molecular imaging and

allowing a better understanding of host-pathogen interactions in several tumor processes. Some studies have reported the pro-carcinogenic activities of *pks*-positive *E. coli* in murine models^[26,33,34]. Most of these studies required animal sacrifice and did not allow longitudinal investigation. Ideally, it would be useful to non-invasively, longitudinally monitor these procarcinogenic processes. Here, we report the first study that utilized optical imaging in these settings. More precisely, we focused on CRC carcinogenesis and pathogenic *E. coli* association.

We described a specific accumulation of the 2-deoxyglucosone fluorescent probe to the tumor site (CRC xenograft model), thus establishing a correlation between tumor volume and fluorescent signal intensity. We showed that this method provides an effective tool to assess longitudinal data on CRC tumor growth *in vivo*. Moreover, in our experimental conditions, xenografts infected with *pks*-positive *E. coli* exhibited comparable development to uninfected ones, confirming results reported for the same experimental conditions by Cougnoux *et al.*^[34]. However, they observed a significant increase in tumor volume induced by colibactin, starting from day 44 after the xenograft. In the present study, we chose to evaluate inflammation and ROS production at an early stage, before the effect of colibactin on tumor cells proliferation. Indeed, Arthur *et al.*^[39] suggested that inflammation is necessary for *E. coli*'s cancer-promoting activity, probably through the enhancement of its resilience among gut microbiota in the intestine. Our results showed that the BLI signal significantly increases with bacterial infection. Pathogenic *E. coli* seemed to enhance inflammation and ROS production, which could participate in carcinogenesis. Using luminol-based BLI, we showed that *pks*-positive *E. coli* induced oxidative stress, which is involved in carcinogenesis process. We confirmed this observation on histological examination, which showed that inflammatory cells were mostly recruited in infected xenografts. Tumor necrosis also appeared in the *pks*-positive *E. coli* group. Moreover, a significant increase of MPO activity, which led to ROS production by infiltrating immune cells, was confirmed with an ELISA on HCT116-cells tumor specimens. Finally, these data showed that *pks*-positive-*E. coli* induced inflammation and ROS production at an early stage after infection, and could thus be an important mechanism involved in pro-carcinogenic activity.

To validate the use of luminol-based BLI imaging to monitor inflammation and oxidative stress, we used an *in vivo* colitis model (CEABAC10/DSS). We proved that monitoring inflammation in deep tissues is feasible and effective. This suggests that optical imaging should be tested on other murine models (APC^{min/+}, AOM-IL10^{-/-}, AOM-DSS) used to determine the pro-carcinogenic properties of *pks*-positive *E. coli* strains, and it may facilitate a better understanding of how pathogenic bacteria impact the carcinogenesis process by various

mechanisms. Using CEABAC10 models mimicking Crohn's disease, we suggest that optical imaging is an effective method in inflammatory bowel disease research.

In conclusion, by using optical imaging, particularly the BLI approach, we provided additional tools to better understand host-pathogen interactions in digestive pathology, including CRC and inflammatory bowel disease.

COMMENTS

Background

Colorectal carcinoma (CRC) is a complex association of non-neoplastic and tumoral cells and a large amount of microorganisms. *Escherichia coli* (*E. coli*) is a consistent commensal of the human gut microbiota but some pathogenic strains have acquired the ability to produce toxins as cyclomodulins that can interfere with eukaryotic cell cycle or directly induce DNA damages. It was observed that cyclomodulin-producing-*E. coli* are more frequently detected on CRC patients and exhibit procarcinogenic properties on murine models.

Research frontiers

Novel imaging techniques like optical imaging could be a powerful tool in translational cancer. Particularly, *in vivo* optical imaging is an innovative tool for non-invasive, spatiotemporal and quantitative monitoring of carcinogenesis process in murine models. It may help to better understand the host-pathogen interactions in colorectal tumor development.

Innovations and breakthroughs

This study investigates the *in vivo* mechanisms of epithelial colonic mucosa infection by cyclomodulin-positive-*E. coli*. Because chronic inflammation and reactive oxygen species (ROS) production are key factors in bacteria and CRC interactions, the authors choose to evaluate cyclomodulin-positive-*E. coli* infection on these mechanisms using optical imaging and commercial, available and validated probes. By using this technique, the authors provided tools to better understand host-pathogen interactions on murine models at the early stage of disease, such as inflammatory bowel disease and CRC.

Applications

By using optical imaging, particularly the bioluminescent approach, the authors provided additional tools to better understand host-pathogen interactions in digestive pathology, including CRC and inflammatory bowel disease. The data suggest that cyclomodulin-positive-*E. coli* induced inflammation and ROS production at an early stage after infection, and could thus be an important mechanism involved in pro-carcinogenic activity of these bacteria.

Terminology

Oxidative stress reflects an imbalance between the systemic manifestation of ROS and the cellular biological system's ability to readily detoxify the reactive intermediates or to repair the resulting damage. Disturbances in the normal redox state of cells can cause toxic effects through the production of peroxides and free radicals that damage all components of the cell, including proteins, lipids, and DNA. In humans, oxidative stress is thought to be involved in the development of several cancers.

Peer-review

Good interesting novel study. The experiments were well designed.

REFERENCES

- 1 Ferlay J, Soerjomataram I, Dikshit R, Eser S, Mathers C, Rebelo M, Parkin DM, Forman D, Bray F. Cancer incidence and mortality worldwide: sources, methods and major patterns in GLOBOCAN 2012. *Int J Cancer* 2015; **136**: E359-E386 [PMID: 25220842 DOI:

- 10.1002/ijc.29210]
- 2 **Ferlay J**, Shin HR, Bray F, Forman D, Mathers C, Parkin DM. Estimates of worldwide burden of cancer in 2008: GLOBOCAN 2008. *Int J Cancer* 2010; **127**: 2893-2917 [PMID: 21351269 DOI: 10.1002/ijc.25516]
 - 3 **Fearon ER**, Vogelstein B. A genetic model for colorectal tumorigenesis. *Cell* 1990; **61**: 759-767 [PMID: 2188735 DOI: 10.1016/0092-8674(90)90186-I]
 - 4 **Collins D**, Hogan AM, Winter DC. Microbial and viral pathogens in colorectal cancer. *Lancet Oncol* 2011; **12**: 504-512 [PMID: 21067973 DOI: 10.1016/S1470-2045(10)70186-8]
 - 5 **de Martel C**, Ferlay J, Franceschi S, Vignat J, Bray F, Forman D, Plummer M. Global burden of cancers attributable to infections in 2008: a review and synthetic analysis. *Lancet Oncol* 2012; **13**: 607-615 [PMID: 22575588 DOI: 10.1016/S1470-2045(12)70137-7]
 - 6 **Parsonnet J**, Friedman GD, Vandersteeen DP, Chang Y, Vogelman JH, Orentreich N, Sibley RK. Helicobacter pylori infection and the risk of gastric carcinoma. *N Engl J Med* 1991; **325**: 1127-1131 [PMID: 1891020 DOI: 10.1056/NEJM199110173251603]
 - 7 **Irrazabal T**, Belcheva A, Girardin SE, Martin A, Philpott DJ. The multifaceted role of the intestinal microbiota in colon cancer. *Mol Cell* 2014; **54**: 309-320 [PMID: 24766895 DOI: 10.1016/j.molcel.2014.03.039]
 - 8 **Sears CL**, Garrett WS. Microbes, microbiota, and colon cancer. *Cell Host Microbe* 2014; **15**: 317-328 [PMID: 24629338 DOI: 10.1016/j.chom.2014.02.007]
 - 9 **Tjalsma H**, Boleij A, Marchesi JR, Dutilh BE. A bacterial driver-passenger model for colorectal cancer: beyond the usual suspects. *Nat Rev Microbiol* 2012; **10**: 575-582 [PMID: 22728587 DOI: 10.1038/nrmicro2819]
 - 10 **Jobin C**. Microbial dysbiosis, a new risk factor in colorectal cancer?. *Med Sci (Paris)* 2013; **29**: 582-585 [PMID: 23859512 DOI: 10.1051/medsci/2013296010]
 - 11 **Sobhani I**, Amiot A, Le Baleur Y, Levy M, Auriault ML, Van Nhieu JT, Delchier JC. Microbial dysbiosis and colon carcinogenesis: could colon cancer be considered a bacteria-related disease? *Therap Adv Gastroenterol* 2013; **6**: 215-229 [PMID: 23634186 DOI: 10.1177/1756283X12473674]
 - 12 **Gao Z**, Guo B, Gao R, Zhu Q, Qin H. Microbiota disbiosis is associated with colorectal cancer. *Front Microbiol* 2015; **6**: 20 [PMID: 25699023 DOI: 10.3389/fmicb.2015.00020]
 - 13 **Sobhani I**, Tap J, Roudot-Thoraval F, Roperch JP, Letulle S, Langella P, Corthier G, Tran Van Nhieu J, Furet JP. Microbial dysbiosis in colorectal cancer (CRC) patients. *PLoS One* 2011; **6**: e16393 [PMID: 21297998 DOI: 10.1371/journal.pone.0016393]
 - 14 **Abdulmir AS**, Hafidh RR, Abu Bakar F. The association of Streptococcus bovis/galloyticus with colorectal tumors: the nature and the underlying mechanisms of its etiological role. *J Exp Clin Cancer Res* 2011; **30**: 11 [PMID: 21247505 DOI: 10.1186/1756-9966-30-11]
 - 15 **Klein RS**, Recco RA, Catalano MT, Edberg SC, Casey JJ, Steigbigel NH. Association of Streptococcus bovis with carcinoma of the colon. *N Engl J Med* 1977; **297**: 800-802 [PMID: 408687 DOI: 10.1056/NEJM197710132971503]
 - 16 **Balamurugan R**, Rajendiran E, George S, Samuel GV, Ramakrishna BS. Real-time polymerase chain reaction quantification of specific butyrate-producing bacteria, Desulfovibrio and Enterococcus faecalis in the feces of patients with colorectal cancer. *J Gastroenterol Hepatol* 2008; **23**: 1298-1303 [PMID: 18624900 DOI: 10.1111/j.1440-1746.2008.05490]
 - 17 **Grahn N**, Hmani-Aifa M, Fransén K, Söderkvist P, Monstein HJ. Molecular identification of Helicobacter DNA present in human colorectal adenocarcinomas by 16S rDNA PCR amplification and pyrosequencing analysis. *J Med Microbiol* 2005; **54**: 1031-1035 [PMID: 16192433 DOI: 10.1099/jmm.0.46122-0]
 - 18 **Jones M**, Helliwell P, Pritchard C, Tharakan J, Mathew J. Helicobacter pylori in colorectal neoplasms: is there an aetiological relationship? *World J Surg Oncol* 2007; **5**: 51 [PMID: 17498313 DOI: 10.1186/1477-7819-5-51]
 - 19 **Zumkeller N**, Brenner H, Zwahlen M, Rothenbacher D. Helicobacter pylori infection and colorectal cancer risk: a meta-analysis. *Helicobacter* 2006; **11**: 75-80 [PMID: 16579836 DOI: 10.1111/j.1523-5378.2006.00381.x]
 - 20 **Housseau F**, Sears CL. Enterotoxigenic Bacteroides fragilis (ETBF)-mediated colitis in Min (Apc+/-) mice: a human commensal-based murine model of colon carcinogenesis. *Cell Cycle* 2010; **9**: 3-5 [PMID: 20009569]
 - 21 **Toprak NU**, Yagci A, Gulluoglu BM, Akin ML, Demirkalem P, Celenk T, Soyletir G. A possible role of Bacteroides fragilis enterotoxin in the aetiology of colorectal cancer. *Clin Microbiol Infect* 2006; **12**: 782-786 [PMID: 16842574 DOI: 10.1111/j.1469-0691.2006.01494.x]
 - 22 **Mirza NN**, McCloud JM, Cheetham MJ. Clostridium septicum sepsis and colorectal cancer - a reminder. *World J Surg Oncol* 2009; **7**: 73 [PMID: 19807912 DOI: 10.1186/1477-7819-7-73]
 - 23 **McCoy AN**, Araújo-Pérez F, Azcárate-Peril A, Yeh JJ, Sandler RS, Keku TO. Fusobacterium is associated with colorectal adenomas. *PLoS One* 2013; **8**: e53653 [PMID: 23335968 DOI: 10.1371/journal.pone.0053653]
 - 24 **Rubinstein MR**, Wang X, Liu W, Hao Y, Cai G, Han YW. Fusobacterium nucleatum promotes colorectal carcinogenesis by modulating E-cadherin/β-catenin signaling via its FadA adhesin. *Cell Host Microbe* 2013; **14**: 195-206 [PMID: 23954158 DOI: 10.1016/j.chom.2013.07.012]
 - 25 **Swidsinski A**, Khilkin M, Kerjaschki D, Schreiber S, Ortner M, Weber J, Lochs H. Association between intraepithelial Escherichia coli and colorectal cancer. *Gastroenterology* 1998; **115**: 281-286 [PMID: 9679033]
 - 26 **Arthur JC**, Perez-Chanona E, Mühlbauer M, Tomkovich S, Uronis JM, Fan TJ, Campbell BJ, Abujamel T, Dogan B, Rogers AB, Rhodes JM, Stintzi A, Simpson KW, Hansen JJ, Keku TO, Fodor AA, Jobin C. Intestinal inflammation targets cancer-inducing activity of the microbiota. *Science* 2012; **338**: 120-123 [PMID: 22903521 DOI: 10.1126/science.1224820]
 - 27 **Leser TD**, Mølbak L. Better living through microbial action: the benefits of the mammalian gastrointestinal microbiota on the host. *Environ Microbiol* 2009; **11**: 2194-2206 [PMID: 19737302 DOI: 10.1111/j.1462-2920.2009.01941.x]
 - 28 **Nougayrède JP**, Homburg S, Taieb F, Boury M, Brzuszkiewicz E, Gottschalk G, Buchrieser C, Hacker J, Dobrindt U, Oswald E. Escherichia coli induces DNA double-strand breaks in eukaryotic cells. *Science* 2006; **313**: 848-851 [PMID: 16902142 DOI: 10.1126/science.1127059]
 - 29 **Cuevas-Ramos G**, Petit CR, Marcq I, Boury M, Oswald E, Nougayrède JP. Escherichia coli induces DNA damage in vivo and triggers genomic instability in mammalian cells. *Proc Natl Acad Sci USA* 2010; **107**: 11537-11542 [PMID: 20534522 DOI: 10.1073/pnas.1001261107]
 - 30 **Buc E**, Dubois D, Sauvanet P, Raisch J, Delmas J, Darfeuille-Michaud A, Pezet D, Bonnet R. High prevalence of mucosa-associated E. coli producing cyclomodulin and genotoxin in colon cancer. *PLoS One* 2013; **8**: e56964 [PMID: 23457644 DOI: 10.1371/journal.pone.0056964]
 - 31 **Arthur JC**, Jobin C. The complex interplay between inflammation, the microbiota and colorectal cancer. *Gut Microbes* 2013; **4**: 253-258 [PMID: 23549517 DOI: 10.4161/gmic.24220]
 - 32 **Prorok-Hamon M**, Friswell MK, Alswied A, Roberts CL, Song F, Flanagan PK, Knight P, Codling C, Marchesi JR, Winstanley C, Hall N, Rhodes JM, Campbell BJ. Colonic mucosa-associated diffusely adherent afaC+ Escherichia coli expressing lpfA and pks are increased in inflammatory bowel disease and colon cancer. *Gut* 2014; **63**: 761-770 [PMID: 23846483 DOI: 10.1136/gutjnl-2013-304739]
 - 33 **Bonnet M**, Buc E, Sauvanet P, Darcha C, Dubois D, Pereira B, Déchelotte P, Bonnet R, Pezet D, Darfeuille-Michaud A. Colonization of the human gut by E. coli and colorectal cancer risk. *Clin Cancer Res* 2014; **20**: 859-867 [PMID: 24334760 DOI: 10.1158/1078-0432.CCR-13-1343]
 - 34 **Cougnoux A**, Dalmasso G, Martinez R, Buc E, Delmas J, Gibold L, Sauvanet P, Darcha C, Déchelotte P, Bonnet M, Pezet D, Wodrich

- H, Darfeuille-Michaud A, Bonnet R. Bacterial genotoxin colibactin promotes colon tumour growth by inducing a senescence-associated secretory phenotype. *Gut* 2014; **63**: 1932-1942 [PMID: 24658599 DOI: 10.1136/gutjnl-2013-305257]
- 35 **Razkin J**, Josserand V, Boturyn D, Jin ZH, Dumy P, Favrot M, Coll JL, Texier I. Activatable fluorescent probes for tumour-targeting imaging in live mice. *ChemMedChem* 2006; **1**: 1069-1072 [PMID: 16944544 DOI: 10.1002/cmdc.200600118]
- 36 **Riedel SS**, Mottok A, Brede C, Bäuerlein CA, Jordán Garrote AL, Ritz M, Mattenheimer K, Rosenwald A, Einsele H, Bogen B, Beilhack A. Non-invasive imaging provides spatiotemporal information on disease progression and response to therapy in a murine model of multiple myeloma. *PLoS One* 2012; **7**: e52398 [PMID: 23300660]
- 37 **Jenkins DE**, Oei Y, Hornig YS, Yu SF, Dusich J, Purchio T, Contag PR. Bioluminescent imaging (BLI) to improve and refine traditional murine models of tumor growth and metastasis. *Clin Exp Metastasis* 2003; **20**: 733-744 [PMID: 14713107]
- 38 **Raisch J**, Rolhion N, Dubois A, Darfeuille-Michaud A, Bringer MA. Intracellular colon cancer-associated *Escherichia coli* promote protumoral activities of human macrophages by inducing sustained COX-2 expression. *Lab Invest* 2015; **95**: 296-307 [PMID: 25545478 DOI: 10.1038/labinvest.2014]
- 39 **Arthur JC**, Gharaibeh RZ, Mühlbauer M, Perez-Chanona E, Uronis JM, McCafferty J, Fodor AA, Jobin C. Microbial genomic analysis reveals the essential role of inflammation in bacteria-induced colorectal cancer. *Nat Commun* 2014; **5**: 4724 [PMID: 25182170 DOI: 10.1038/ncomms5724]
- 40 **Maddocks OD**, Short AJ, Donnenberg MS, Bader S, Harrison DJ. Attaching and effacing *Escherichia coli* downregulate DNA mismatch repair protein in vitro and are associated with colorectal adenocarcinomas in humans. *PLoS One* 2009; **4**: e5517 [PMID: 19436735 DOI: 10.1371/journal.pone.0005517]
- 41 **Darfeuille-Michaud A**, Boudeau J, Bulois P, Neut C, Glasser AL, Barnich N, Bringer MA, Swidsinski A, Beaugerie L, Colombel JF. High prevalence of adherent-invasive *Escherichia coli* associated with ileal mucosa in Crohn's disease. *Gastroenterology* 2004; **127**: 412-421 [PMID: 15300573 DOI: 10.1053/j.gastro.2004.04.061]
- 42 **Manichanh C**, Borruel N, Casellas F, Guarner F. The gut microbiota in IBD. *Nat Rev Gastroenterol Hepatol* 2012; **9**: 599-608 [PMID: 22907164 DOI: 10.1038/nrgastro.2012.152]
- 43 **Maddocks OD**, Scanlon KM, Donnenberg MS. An *Escherichia coli* effector protein promotes host mutation via depletion of DNA mismatch repair proteins. *MBio* 2013; **4**: e00152-e00113 [PMID: 23781066 DOI: 10.1128/mBio.00152-13]
- 44 **Gross S**, Gammon ST, Moss BL, Rauch D, Harding J, Heinecke JW, Ratner L, Piwnica-Worms D. Bioluminescence imaging of myeloperoxidase activity in vivo. *Nat Med* 2009; **15**: 455-461 [PMID: 19305414 DOI: 10.1038/nm.1886]
- 45 **Alshetaiwi HS**, Balivada S, Shrestha TB, Pyle M, Basel MT, Bossmann SH, Troyer DL. Luminol-based bioluminescence imaging of mouse mammary tumors. *J Photochem Photobiol B* 2013; **127**: 223-228 [PMID: 24077442 DOI: 10.1016/j.jphotobiol.2013.08.017]
- 46 **Denizot J**, Sivignon A, Barreau F, Darcha C, Chan HF, Stanners CP, Hofman P, Darfeuille-Michaud A, Barnich N. Adherent-invasive *Escherichia coli* induce claudin-2 expression and barrier defect in CEABAC10 mice and Crohn's disease patients. *Inflamm Bowel Dis* 2012; **18**: 294-304 [PMID: 21688348 DOI: 10.1002/ibd.21787]

P- Reviewer: Cao GW, Erem HH, Kodaz H **S- Editor:** Gong XM

L- Editor: A **E- Editor:** Wu HL





Published by **Baishideng Publishing Group Inc**

8226 Regency Drive, Pleasanton, CA 94588, USA

Telephone: +1-925-223-8242

Fax: +1-925-223-8243

E-mail: bpgoffice@wjgnet.com

Help Desk: <http://www.wjgnet.com/esps/helpdesk.aspx>

<http://www.wjgnet.com>

